Autofluorescence in Plants

Lloyd Donaldson

Scion, Private Bag 3020, Rotorua 3046, New Zealand; lloyd.donaldson@scionresearch.com; Tel.: +64-7-343-5581

Abstract: Plants contain abundant autofluorescent molecules that can be used for biochemical, physiological, or imaging studies. The two most studied molecules are chlorophyll (orange/red fluorescence) and lignin (blue/green fluorescence). Chlorophyll fluorescence is used to measure the physiological state of plants using handheld devices that can measure photosynthesis, linear electron flux, and CO_2 assimilation by directly scanning leaves, or by using reconnaissance imaging from a drone, an aircraft or a satellite. Lignin fluorescence can be used in imaging studies of wood for phenotyping of genetic variants in order to evaluate reaction wood formation, assess chemical modification of wood, and study fundamental cell wall properties using Förster Resonant Energy Transfer (FRET) and other methods. Many other fluorescent molecules have been characterized both within the protoplast and as components of cell walls. Such molecules have fluorescence emissions across the visible spectrum and can potentially be differentiated by spectral imaging or by evaluating their response to change in pH (ferulates) or chemicals such as Naturstoff reagent (flavonoids). Induced autofluorescence using glutaraldehyde fixation has been used to enable imaging of proteins/organelles in the cell protoplast and to allow fluorescence imaging of fungal mycelium.
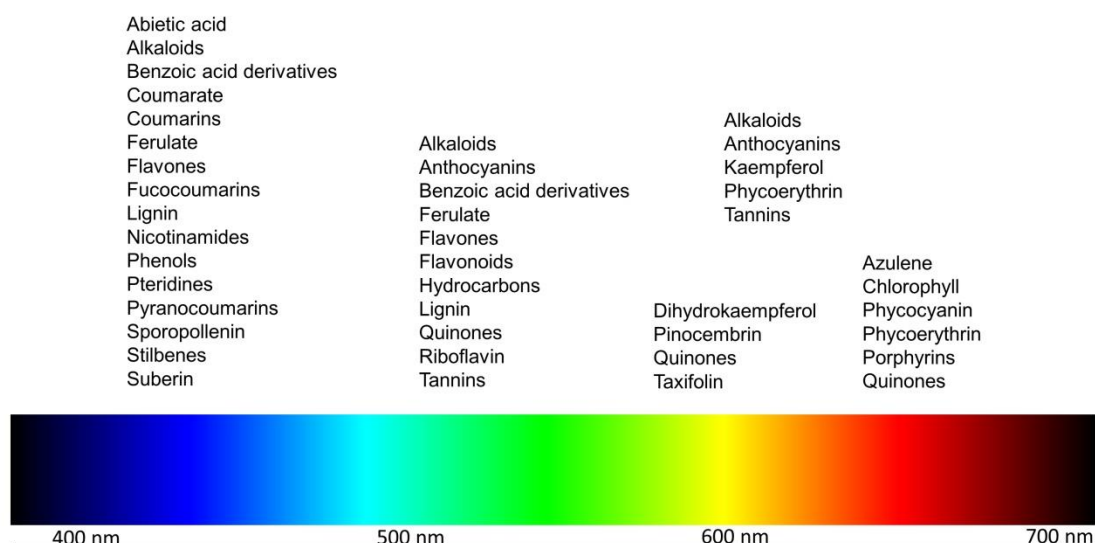
Keywords: autofluorescence; chlorophyll; lignin; suberin; phenolic acids; flavonoids; tannins; FLIM; FRET; spectral unmixing

1. Introduction

Autofluorescent molecules are common in plant tissues [1]. This can be viewed from two opposing perspectives. Autofluorescence can be considered problematic [2–4]—autofluorescent molecules may interfere with the detection of fluorescent staining, reporter molecules such as GFP (green fluorescent protein), or with immunolocalization techniques. Alternatively, autofluorescence can be used as a label-free method for detecting specific molecules using spectral fluorescence imaging techniques and hence can be considered advantageous for some experimental investigations [1,5–12]. Molecular microscopy using F-techniques (Förster Resonant Energy Transfer (FRET), Fluorescence Lifetime Imaging (FLIM), Fluorescence Recovery after Photobleaching (FRAP), and Fluorescence Correlation Spectroscopy (FCS)) is a growing field of investigation in plant biochemistry, physiology, and pathology and in biomaterial characterization. The two most important autofluorescent molecules found in plants are chlorophyll and lignin but a wide range of other molecules are also autofluorescent with UV or visible excitation including components of both cytoplasm and cell walls (Figure 1) [1].

When investigating autofluorescence in plant tissues, it is important to recognize there may be several types of autofluorescent molecules present at the same location and thus the source of autofluorescence should be interpreted in conjunction with histochemical staining and other forms of analysis [13]. For microscopy applications, autofluorescence should be examined on fresh tissue as some autofluorescent compounds (chlorophyll, flavonoids) can easily become redistributed or be completely removed from tissue when exposed to solvent-based fixatives such as formalin aceto-alcohol (FAA) or mounting media such as glycerol—instead, aqueous buffers can be used as mounting media [14,15].
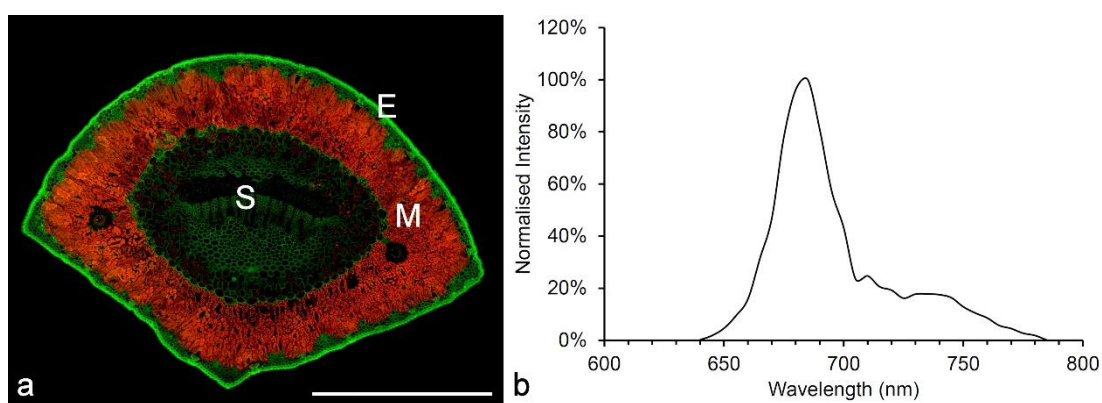
Plant autofluorescence

Abietic acid
Alkaloids
Benzoic acid derivatives
Coumarate
Coumarins
Ferulate   Alkaloids
Flavones   Anthocyanins
Fucocoumarins Benzoic acid derivatives
Lignin   Ferulate
Nicotinamides   Flavones
Phenols   Flavonoids
Pteridines   Hydrocarbons
Pyranocoumarins Lignin
Sporopollenin Quinones
Stilbenes   Riboflavin
Suberin   Tannins

Alkaloids
Anthocyanins
Kaempferol
Phycoerythrin
Tannins

Azulene
Chlorophyll
Dihydrokaempferol Phycocyanin
Pinocembrin   Phycoerythrin
Quinones   Porphyrins
Taxifolin   Quinones

400 nm   500 nm   600 nm   700 nm

Figure 1. Fluorescence emission of common autofluorescent compounds found in plants [1–15].

2. Chlorophyll and Other Pigments

Chlorophyll autofluorescence is used both in lab-scale experiments and in remote sensing applications to evaluate plant health/vigor by directly measuring photosynthetic efficiency and has become a key technique for evaluating the response of plants to changes in the environment [16,17]. Chlorophyll is excited by UV, blue or green light and emits strongly in the red with a distinct bimodal emission with maxima at 685 and 720–730 nm (Figure 2) [16].

Figure 2. Autofluorescence of chlorophyll in leaves. (**a**) A transverse section (TS) of a pine needle showing autofluorescence of chlorophyll (red) in the mesophyll tissue (M) (excitation at 488 and 561 nm, emission at 500–569, 570–700 nm). The bright green fluorescence in the epidermis (E) originates from flavonoids bound to the cell wall, while the weaker green fluorescence in the stele (S) represents lignin. Scale bar = 500 μm. (**b**) The fluorescence spectrum of pine chlorophyll (excitation at 561 nm, emission at 600–800 nm) [15].

All chlorophyll molecules possess extensive conjugated bonds in the form of a porphyrin ring that are responsible for the fluorescence (Figure 3) [16].

Chlorophyll
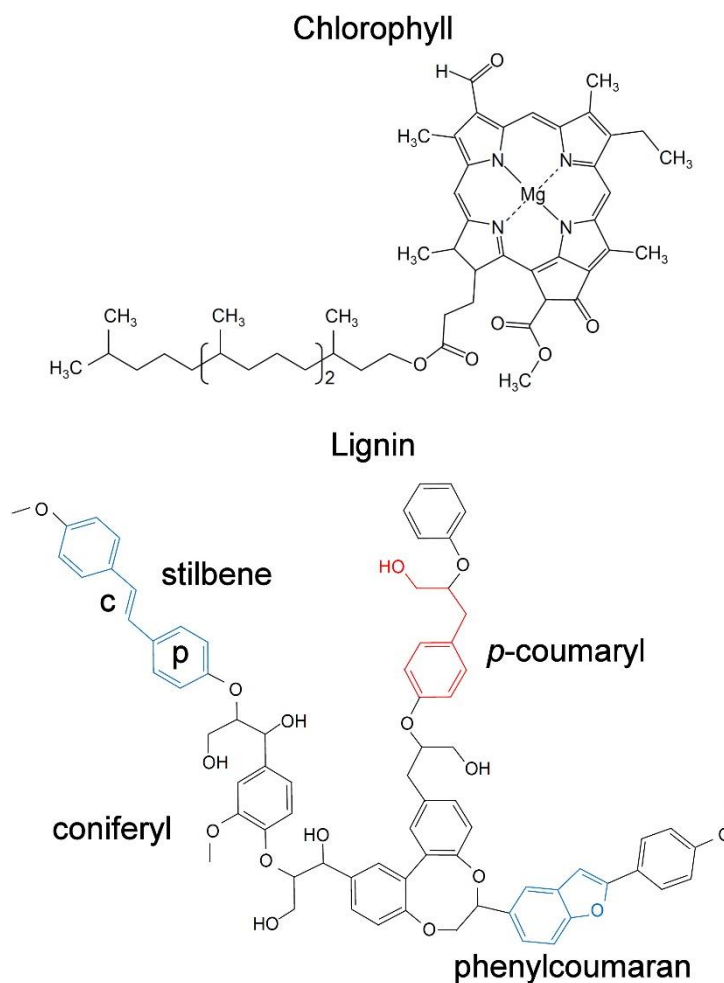
Lignin

Figure 3. The molecular structure of chlorophyll and lignin to illustrate typical fluorescent structures. Chlorophyll contains a large complex porphyrin ring structure accounting for most of its fluorescence. However, chlorophyll molecules within chloroplasts occur in ordered arrays called photosystems which are also likely to influence the fluorescence. Lignin forms a large complex molecule—only a fraction of which is shown here. Structural components that may contribute to the overall fluorescence of lignin are highlighted including phenolic rings (p) and conjugated bonds (c). These types of structures are characteristic of organic fluorophores.

The quantum yield, a measure of the brightness of fluorescence representing the ratio of photons absorbed to emitted, is 0.25 for chlorophyll a in solution and is independent of excitation wavelength or solvent [18]. Because the fluorescence of chlorophyll is a dynamic process in situ, analysis of the spectrum at liquid nitrogen temperatures has been used to obtain more precise spectral information although applications of fluorescence measurement or imaging are usually performed at ambient temperature. Low-temperature spectroscopy has identified a third emission peak at 695 nm [16]. The emission at 685–695 nm is known to be associated with photosystem II, while the broader peak at 720–730 nm is associated with photosystem I [19]. The overall in situ fluorescence of chlorophyll is due to the emission characteristics of both individual chlorophyll molecules and the larger-scale light-harvesting complexes (Figure 3). A characteristic of autofluorescence resulting from multiple emitters within molecules or molecular complexes is the multi-Gaussian model of the emission which can be deconvolved into individual Gaussian (or log-normal) peaks. In the case of chlorophyll, the overall spectrum may contain six Gaussian components with peaks at 680, 685, 695, 700, 720, and 735 nm and these have been associated with various components of photosystem II (680–700 nm) and photosystem I (720–735 nm) [20].

Chlorophyll fluorescence can be used to measure photosynthesis, linear electron flux, and CO_2 assimilation non-destructively in vivo using commercially available portable sensors [21–25]. This allows for the rapid screening of large numbers of plants to evaluate physiological status in relation to genetic and environmental variables. Although the measurement of fluorescence parameters is simple, several corrections need to be applied related to photochemical and non-photochemical quenching [16]. Chlorophyll content can be assessed at the individual cell level in protoplasts by using autofluorescence and flow cytometry [22].

Anthocyanin pigments extracted from red cabbage leaves show autofluorescence with UV excitation resulting in violet to blue emission. Excitation must be below 460 nm to excite autofluorescence. The extraction of such pigments may result in fractions that have different λ_{max} values that are dependent on excitation wavelength [26]. In *Brassica*, anthocyanins have a λ_{max} in the range of 360–530 nm depending on excitation wavelength (300–410 nm) [26], whereas in *Arabidopsis* the λ_{max} is 680 nm, resulting from multiphoton excitation at 860 nm [27]. Anthocyanins, therefore, have broad and variable autofluorescence emission.

Carotenoids (carotenes and xanthophylls) fluoresce with deep UV excitation, making it difficult to detect them in situ within cellular compartments by microscopy [28]. Carotenoids absorb blue light and transfer this energy to adjacent chlorophyll molecules, thus expanding the range of light energy absorption for photosynthesis [29]. This energy transfer does not involve fluorescence emission although very weak autofluorescence at 560 nm has been reported and attributed to carotenoids in green algae [30] and in the range of 400–500 nm in extracts from Persimmon fruit [28].
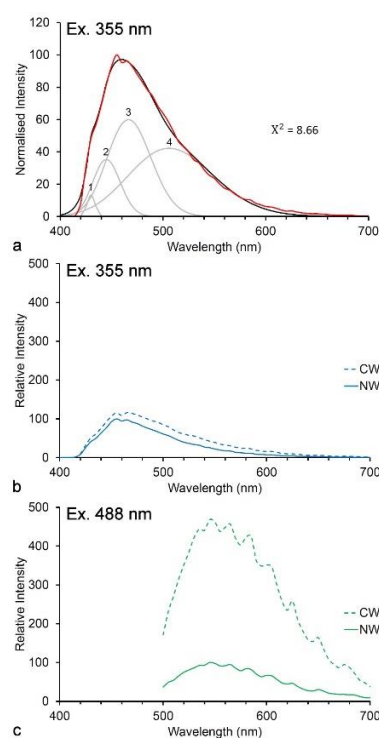
3. Lignin

Lignin is an abundant natural polymer of coniferyl, sinapyl or *p*-coumaryl alcohol that occurs in woody plant tissues, especially in xylem but also in other sclerenchymatous tissues. The interest in lignin autofluorescence is primarily as a means of visualizing lignin microscopically in wood and paper fibers [31]. While there are alternative fluorescent or brightfield stains for lignin, autofluorescence has some advantages from the perspective of increased specificity and label-free imaging as well as in applications for understanding wood nanostructure using techniques such as Förster Resonant Energy Transfer (FRET). Lignin has a characteristically broad emission range due to the presence of multiple fluorophore types within the lignin molecule (Figure 3) and can thus be used with both UV and visible excitation [32,33], providing some flexibility when combined with for example immunohistochemical localization of (non-fluorescent) cell wall carbohydrates such as mannans, xylans and pectins [34]. As with chlorophyll, lignin emission spectra can be deconvolved into multiple log-normal components although these have not been matched to specific fluorescent centers within the complex polymer molecule [35,36]. However, fluorescent model compounds that contain common structures known to occur within lignin polymers have been studied [37–39]. Such studies have identified phenylcoumarone and stilbene structures that may represent lignin fluorophores (Figure 3) [37]. Phenylcoumarones as a pure compound in dioxane solution have quantum yields of 0.57–0.61 but the fluorescence intensity of lignin is likely to be much less than this and is strongly dependent on excitation wavelength (37). Lignin fluorescence may also be influenced by the physical structure of the polymer including clustering of carbonyl groups and restrictions on intramolecular rotation [40]. Studies on model compounds have focused on deep UV-excited fluorophores rather than visible wavelength fluorophores in lignin.

Lignin fluorescence is sensitive to the molecular environment and so can be manipulated with pH and by treatment with quenching agents such as nitrophenol-labeled carbohydrates [32,41]. Heat treatment [41,42] and infiltration with modifying chemicals [43] can also influence lignin autofluorescence. Lignin fluorescence can, therefore, be used as a biosensor for various research investigations such as measurement of cell wall porosity or detection of infiltrating chemicals in wood modification studies.

3.1. Spectroscopy

Lignin absorbs in the UV range with maximum absorbance at 280 nm [44]. Fluorescence from UV excitation has a peak at 360 nm thought to be due to emission from stilbene and phenylcoumarone structures within the lignin molecule [37]. Fluorescence of lignin in its native state may be quenched due to the presence of covalent linkages to hemicellulose. Treatments that break such bonds including photo-degradation, fungal or bacterial decay, as well as chemical treatments such as removal of carbonyl groups all tend to increase the brightness of lignin fluorescence [33]. However, it is difficult to understand the exact sources of fluorescence in lignin because of the complexity of its structure and its occurrence within a natural composite together with (non-fluorescent) carbohydrates. The extraction of lignin from cell walls inevitably alters its structure and hence its fluorescence. Lignin fluorescence also occurs with visible light excitation suggesting potentially multiple fluorescent structures (Figure 4a) [32,33,35,36]. Both UV and visible emission spectra contain multiple log-normal components resulting from conjugated structures [35,36]. It is quite likely that lignin fluorescence results from resonant energy transfer among different structures [37,40]. When excited by blue laser light, lignin fluorescence shows evidence of weak whispering gallery resonance which may also result from resonant energy transfer processes (Figure 4c) [45,46].

Figure 4. Autofluorescence of lignin in pine wood. (**a**) UV-excited blue fluorescence with λ_{max} at 455–465 nm (excitation at 355 nm, emission at 400–700 nm) showing deconvolution with four log-normal components and a good fit between actual (red) and modeled (black) spectra ($X^2 = 8.66$, ns). (**b**) Autofluorescence (excitation at 355 nm) of normal (NW) and compression wood (CW) lignin in pine showing a negligible brightness difference. (**c**) Autofluorescence (excitation at 488 nm) of normal and compression wood lignin in pine showing the much brighter green fluorescence reflecting an increased quantum yield in compression wood resulting from blue excitation due to increased *p*-hydroxy lignin units. The blue-excited spectrum shows some evidence of resonance effects (waviness).

Different lignin types may show small differences in emission spectra (Figure 4b,c). The H-lignin (*p*-hydroxy) found in the middle lamella layer of normal wood and in the secondary wall of compression wood (reaction wood found in leaning stems), contains additional fluorophores, resulting in increased quantum yield at longer wavelengths [35]. While G and S-lignins (guaiacyl and syringyl, respectively)

normally do not show any spectral differences, in the special case of S-lignin in poplar which contains *p*-hydroxybenzoate groups, this allows differentiation between G-rich and S-rich cell types [32].

3.2. Imaging

Lignin fluorescence has been used extensively in imaging studies of wood and paper [31,32]. Using confocal fluorescence microscopy, lignin can be excited with UV (355 nm) or blue (488 nm) light [32]. These two excitations result in slightly different information. The UV-excited emission is similar to that from other phenolic molecules found in plants and has less contrast between the highly lignified middle lamella and less lignified secondary wall of wood fibers. This suggests a stronger influence of evenly distributed chemical groups and less influence of fluorophore abundance and quantum yield. UV-excited lignin fluorescence is, however, more sensitive to the presence of quenching molecules [41]. Blue excitation results in strong contrast between areas of different lignification and is generally much brighter, partly due to the optical properties of the microscope lenses, which makes it more useful for imaging studies (Figure 5) [32]. Lignin autofluorescence is relatively weak compared to detection with lignin stains such as acriflavin but tends to be more specifically related to lignin—acriflavin will stain other cell wall and cytoplasmic (DNA, RNA) components to varying degrees.
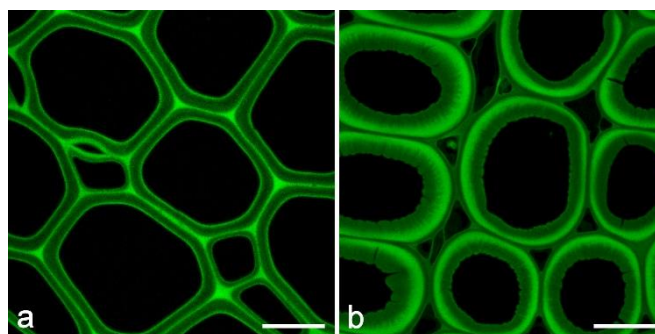
Figure 5. Autofluorescence of lignin in pine wood. (**a**) TS of normal pine wood (excitation at 458 nm, emission at 465–700 nm). Scale bar = 15 μm. (**b**) TS of pine reaction wood showing the altered distribution of lignin (excitation at 458 nm, emission at 465–700 nm). Scale bar = 15 μm.

Lignin autofluorescence has been used to evaluate wood phenotype in radiata pine genetically modified to downregulate the 4-coumarate CoA ligase (4CL) enzyme in the lignin biosynthetic pathway resulting in reduced and variable lignification of tracheid cell walls [47].

Lignin fluorescence in compression wood has been used as a measure of compression wood severity using both spectral analysis and imaging of lignin distribution [35] and has been used to rapidly screen compression wood distribution within trees [48]. Compression wood has undesirable wood properties compared to normal wood including higher shrinkage and lower axial stiffness.

Lignin autofluorescence has been used for colocalization studies showing the distribution of lignin, relative to hemicelluloses (using immunolocalization) and cellulose (using birefringence) in pine wood [34]. Lignin and mannan were shown to be negatively colocalized in both normal and compression wood whereas lignin and galactan were positively colocalized in compression wood but not in normal wood [34]. Similar studies have shown that, in spruce wood, resin canal parenchyma cells with lignified secondary cell walls do not show a reaction wood response (increased lignin and galactan content) compared to adjacent tracheids [49].

Lignin autofluorescence has been used in several studies to assess cell wall porosity. Lignin fluorescence is quenched in the presence of (non-fluorescent) low molecular weight carbohydrates labeled with a nitrophenol group (e.g., 4-nitrophenyl β-D-glucopyranoside). Thus, similar molecules of different molecular weight can be infiltrated into cell walls and their distribution assessed to determine the relative porosity of different cell wall regions [41]. Similar studies using the FRET interaction between lignin (donor)

and rhodamine dye (acceptor) have been used to measure the accessibility of cell wall regions to the dye, demonstrating that highly lignified regions (middle lamella) are less accessible and hence less porous than cellulose-rich regions (secondary cell walls) [50]. These results have been used to optimize methods for the chemical modification of wood cell walls and their infiltration with chemicals used to improve wood properties such as hardness.

Lignocellulosic biomass is a potential source of sustainable biochemicals and liquid biofuels. The presence of lignin inhibits the enzymatic conversion of cellulose by reducing accessibility. There are numerous studies related to the influence of chemical and physical pretreatments designed to mitigate lignin related recalcitrance, many of which use lignin autofluorescence [51–59]. In a study comparing the distribution of fluorescently labeled cellulase enzyme to the distribution of both cellulose and lignin in pretreated woody biomass, lignin autofluorescence was used in combination with Congo red staining of cellulose. This study demonstrated a positive spatial correlation between cellulase enzyme and cellulose, and a negative correlation with lignin distribution [56].

4. Other Cell Wall-Associated Fluorophores

4.1. Ferulate

Ferulic acid may occur in cell walls, where it is usually esterified to polysaccharides, emitting a very weak blue fluorescence with UV excitation at neutral pH that characteristically changes to stronger green emission under conditions of high pH such as in the presence of ammonia (Figure 6) [60]. Ferulic acid is also sensitive to constraint of intramolecular motion, exhibiting an increase in quantum yield (0.0024 to 0.044) when incorporated into rigid biopolymers and hence acting as a biocompatible fluorescent label in biomedical applications [61].
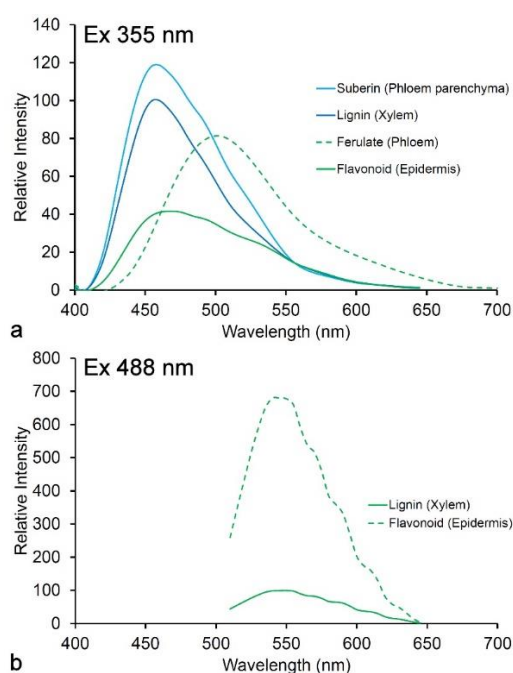
Figure 6. Fluorescence spectra of cell wall autofluorescence in pine needles showing relative brightness. (**a**) Excitation at 350 nm (UV); (**b**) excitation at 488 nm (blue). Flavonoids in the epidermis are much more fluorescent with blue excitation relative to lignin [15].

In conifers, ferulate can be detected in phloem cell walls, especially in the primary wall/middle lamella, with very weak emission in the secondary wall [15,60,62]. There are no histochemical tests for ferulate, so its identification in tissue is based solely on demonstrating a pH-dependent change

from blue to green fluorescence. Other phenolic acids may also produce weak UV-excited blue autofluorescence in cell walls.

4.2. Cutin

The cuticle of plants shows autofluorescence attributed to cutin. The cuticle located on the outer surface of the epidermal cell wall may be of variable thickness among species, only 20–50 nm in *Arabidopsis*, and hence may be difficult to distinguish from the often highly fluorescent epidermal cell wall which is usually very thick (several micrometers). Cutin has a similar fluorescence spectrum to suberin and lignin [63–65]. Studies of cutin-deficient mutants in tomato have been carried out but, unfortunately, autofluorescence was not examined [64]. The exact nature of cutin fluorescence is poorly understood. Cutin is a polyester-based material [66], and fluorescence may originate from phenolic acids or flavonoids bound to the cutin backbone similar to the fluorophores present in the adjacent epidermal cell wall (Figure 6) [15,65].

4.3. Suberin

Suberin, like cutin, is a hydrophobic polyester consisting of long-chain fatty acids and glycerol [67]. It exhibits UV-excited autofluorescence comparable to lignin, from which it can be distinguished by its weak blue-excited autofluorescence relative to lignin (Figure 6) [15,49]. In sequentially UV/blue-excited images, suberin will show violet/blue emission, while lignin will show blue/green emission, although both lignin and suberin may be colocalized and hence indistinguishable in some tissues (endodermis, epidermis, Casparian strips).

4.4. Sporopollenin

Sporopollenin is a chemically inert biopolymer found in the outer layer of spores and pollen. It is composed of aliphatic-polyketide-derived polyvinyl alcohol units and 7-*O*-*p*-coumaroylated C16 aliphatic units [68]. The outer wall of pollen grains and fern spores is autofluorescent, with emission at both blue and yellow wavelengths assumed to be due in part to sporopollenin [69], although other potential fluorophores including pigments such as carotene, flavonoids such as naringenin and terpenes such as azulene may also be present [70]. The autofluorescence is known to be variable both during development and between different species [71,72]. Fluorescence spectra of pollen and spores show indications of three fluorescent peaks, at 475, 565, and 675 nm [72]. The consensus seems to be that the UV-excited blue fluorophore in fern spores and pollen grains is sporopollenin while green/yellow fluorescence may be flavonoids or pigments (carotenoids, lipofuscin), but this needs further study, reflecting the complex mixture of potential fluorophores that may be present (Figure 7).
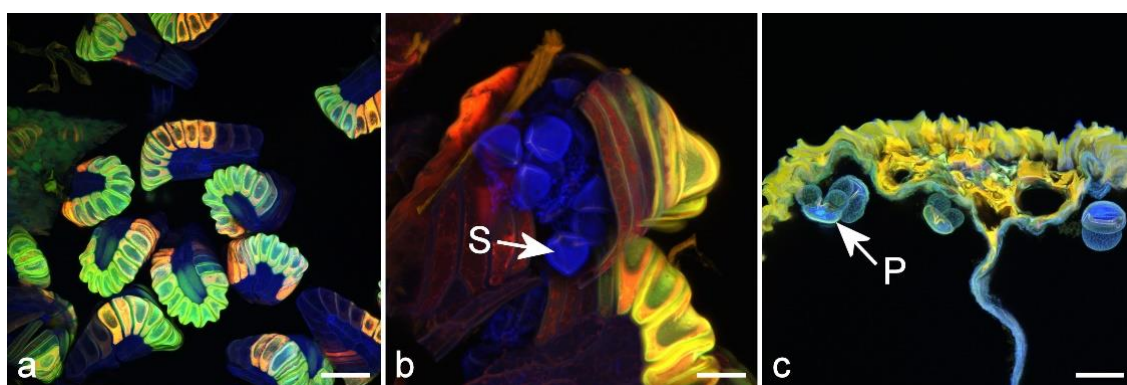
Figure 7. Autofluorescence in reproductive structures. (**a**) Immature fern sporangia. Scale bar = 100 μm. (**b**) Mature sporangium with spores (S). Scale bar = 33 μm. (**c**) TS of a male cone in pine with mature pollen grains (P). Scale bar = 50 μm.

4.5. Flavonoids

Plants contain a wide range of different flavonoids that may be associated with cell walls or may occur as secretions or extractives. A fluorescent flavonoid known as *Lignum nephriticum* (matlaline), the oxidation product of flavonoid extractives from *Eysenhardtia polystachya*, a tropical tree, was first described in the sixteenth century [73]. Flavonoids are of interest as potential therapeutic agents and are autofluorescent with emission at green, yellow and orange wavelengths. This fluorescence can be specifically enhanced by using a reagent containing 2-aminoethyl-diphenylborinate (Naturstoff reagent—DPBA) due to complex formation between DPBA and the flavonoid molecule [74].

Flavonoids are biologically active molecules that occur in plants in more than 10,000 structural variants. Flavonoids have important roles in auxin transport, development of roots and shoots, control of reactive oxygen species, pollination, symbiotic nodule formation, and as defense compounds [75].

Flavonoids (as flavonol glucosides), together with hydroxycinnamic acids and other weakly autofluorescent phenolic materials, are responsible for the fluorescence of the leaf epidermis (Figures 2 and 7) [15,63,76,77].

The autofluorescence properties of flavonoids from paprika have been studied by spectrofluorimetry [78]. Fluorescence intensity was found to increase in high pH medium and multivariate analysis was used to determine optimum excitation and emission characteristics of myricetin, quercetin, and kaempferol. Optimal excitations were in the range of 460–480 nm, with blue and green emission.

The role of flavonoids in auxin transport, gravitropism, and phototropism in mutants of *Arabidopsis* has been investigated using autofluorescence to localize kaempferol, quercetin, and naringenin in root tissues [79,80]. Both kaempferol and quercetin were localized to the nucleus and endomembrane systems of hypocotyl cells.

Flavonoids including dihydrokaempferol, pinocembrin, and taxifolin are major components of extractives in the wood of Douglas-fir occurring within heartwood tracheid cell walls and in resin canals [14]. The fluorescence of extractive deposits has been compared with purified standards allowing identification of different autofluorescent extractive deposits in resin canals and rays (Figure 8).
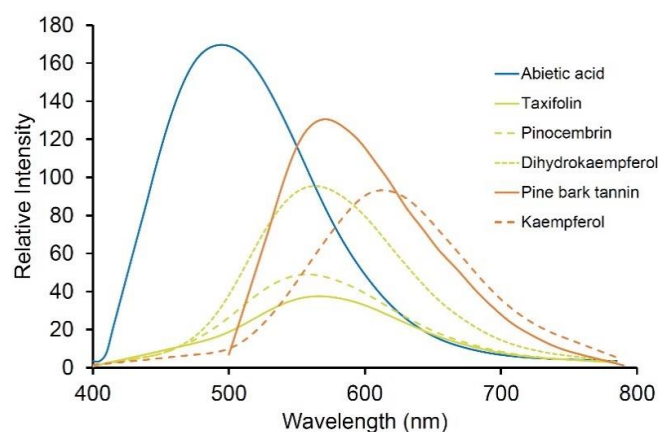
Figure 8. Fluorescence spectra of some common purified wood extractives (from Sigma except for pine bark tannin manufactured by Scion) showing relative brightness [14]. Excitation was at 355 nm except for pine bark tannin which was excited at 488 nm.

5. Other Fluorophores

5.1. Stilbenes

Purified, piceid, pterostilbene and resveratrol show violet emission, with a λ_{max} of 400 nm in water at neutral pH and blue emission at 450–470 nm at high pH. Stilbenes in grape berries were imaged with UV excitation and blue emission and their presence in epidermal vacuoles was associated with reduced susceptibility to downy mildew [81].

5.2. Tannins

Condensed tannins are polymers of catechins generally known as proanthocyanadins. They occur as abundant orange fluorophores in bark and wood (λ_{max} = 565 nm) [82,83] and may also occur in other plant tissues such as leaves and fruit, with fluorescence emissions over the range of 500–650 nm (Figure 8) [84,85].

5.3. Terpenes

The fluorescence of terpenes is variable, with some common terpene extracts such as pinene and limonene being non-fluorescent. Likewise, the triterpene waxes on the surface of fern fronds are non-fluorescent. The exact chemical nature of fluorescence in plant secretory compounds requires more attention as these are more than likely mixtures when they occur in situ within the plant. Azulene is a fluorescent terpenoid that occurs in the secretory cells of plants with emission at red wavelengths [1,10]. This compound is notable as the only known example where fluorescence arises from an upper excited state (S2 → S0) [86]. Resin acids such as abietic acid, a diterpene, are known to be autofluorescent with UV excitation and blue emission (Figure 8). Oleoresins are also weakly autofluorescent with blue emission [14,15].

6. Induced Autofluorescence Using Glutaraldehyde

Treatment of plant tissue with glutaraldehyde will induce or enhance autofluorescence of proteins, so it is a useful method for imaging of cytoplasm in fixed tissue (Figure 9) [63,87,88]. While for some applications this might be problematic, glutaraldehyde fixation can produce excellent images of cytoplasm and can be used for high-resolution confocal fluorescence imaging as opposed to techniques like DIC or phase contrast which are limited to widefield microscopy. Typically, this approach produces a bland yellow autofluorescence (λ_{max} 560 nm) with little or no spectral differentiation but can potentially be combined with fluorescence from other natural fluorophores present within the tissue, or with blue or red-fluorescent dyes for multiple labeling experiments. This method can be particularly useful for imaging fungal hyphae which are difficult to label with fluorescent stains (Figure 9). Fungal hyphae and spores may also show some natural autofluorescence [89].
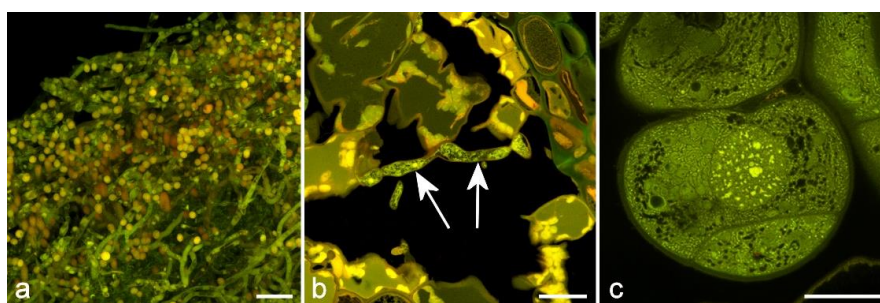
Figure 9. Glutaraldehyde-induced autofluorescence of plant tissues. (**a**) TS of *Penicillium* in culture showing hyphae and spores. Scale bar = 10 μm; (**b**) Pine needle infected with *Phytopthora pluvialis* (arrows). Scale bar = 20 μm. (**c**) Pine somatic embryo using Super-Resolution Radial Fluctuation (SRRF) microscopy [90], showing dense cytoplasm with mitochondria, endoplasmic reticulum, nucleoli, and Golgi vesicles. Scale bar = 10 μm.

7. Deep UV Excitation

Some autofluorescent compounds absorb and emit at shorter wavelengths below the visible part of the spectrum—amino acids such as tryptophan, for example. While measuring fluorescence spectra of materials extracted from plants is straightforward at these excitation wavelengths, in situ spectroscopy and imaging are difficult at deep UV excitation wavelengths due to the lack of suitable lasers (for confocal fluorescence imaging) as well as limitations in the characteristics of lenses. Deep UV fluorescence images will be heavily shaded—that is, the emission may be uneven due to inhomogeneity

of illumination at short wavelengths. Nevertheless, some imaging studies have been performed on plant tissues in situ using synchrotron radiation for excitation to localize protein (cellulase enzyme) and phenolic residues [91,92].

8. Spectral Imaging and Unmixing

8.1. Sequential Excitation/Emission Imaging

Since plant tissues may contain multiple autofluorescent compounds, it is often of interest to produce images that show their relative locations [14,15]. Imaging with a single excitation and a single emission band only detects total fluorescence as well as spatial variation in intensity (Figure 5). This provides limited information on the spatial distribution of multiple fluorophores. Instead, using one or more excitation wavelengths and multiple emission bands will produce a color image by assigning blue, green, and red to the emission bands, providing some spectral separation of potentially many different fluorophores (Figures 10 and 11) [63]. The most effective way of doing this is to sequentially acquire each emission band using only a single excitation wavelength at a time. On filter-based fluorescence microscopes, this is very slow because of the need to physically move filter wheels and dichroic mirrors during the acquisition. However, AOTF/AOBS-based systems (acousto-optical tunable filter and acousto-optical beam splitter) electronically change the excitation/emission signals, allowing sequential acquisition line by line in real-time rather than the tedious frame by frame serial acquisition required for filter-based instruments. Sequential imaging allows potential overlap of excitation and emission bands and eliminates bleed-through between emission bands. Bleed-through occurs when emission from a shorter wavelength excitation is detected in the emission channel of a second longer wavelength excitation when the two excitations are applied simultaneously. This can easily be demonstrated by removing the shorter wavelength excitation and observing a reduction in brightness of the longer wavelength emission channel.
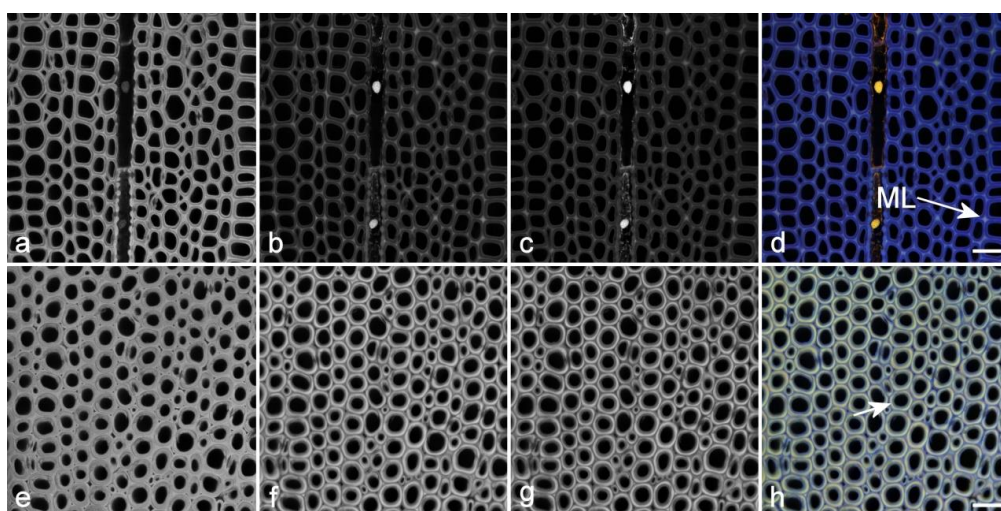
Figure 10. Spectral imaging of lignin autofluorescence using sequential excitation with emission ranges centered around the λ_{max} for each excitation wavelength at a constant gain. Excitation at 355 nm (UV) (**a**,**e**), 488 nm (blue) (**b**,**f**) and 561 nm (green) (**c**,**g**). Color overlays are shown in (**d**,**h**). (**a**–**d**) Normal pine wood showing monochromatic lignin fluorescence at UV, blue and green excitations. Scale bar = 30 μm. (**e**,**h**) Pine compression wood showing the same range of excitation and emission highlighting the change in lignin distribution in this wood type compared to normal wood. UV excitation shows the same intensity, whereas blue and green excitations are significantly brighter compared to normal wood (images of normal and compression wood were acquired at the same gain). Blue and green excitation clearly show the more lignified middle lamella (ML) and outer secondary cell wall (short arrow) in the two specimens respectively. Scale bar = 30 μm.
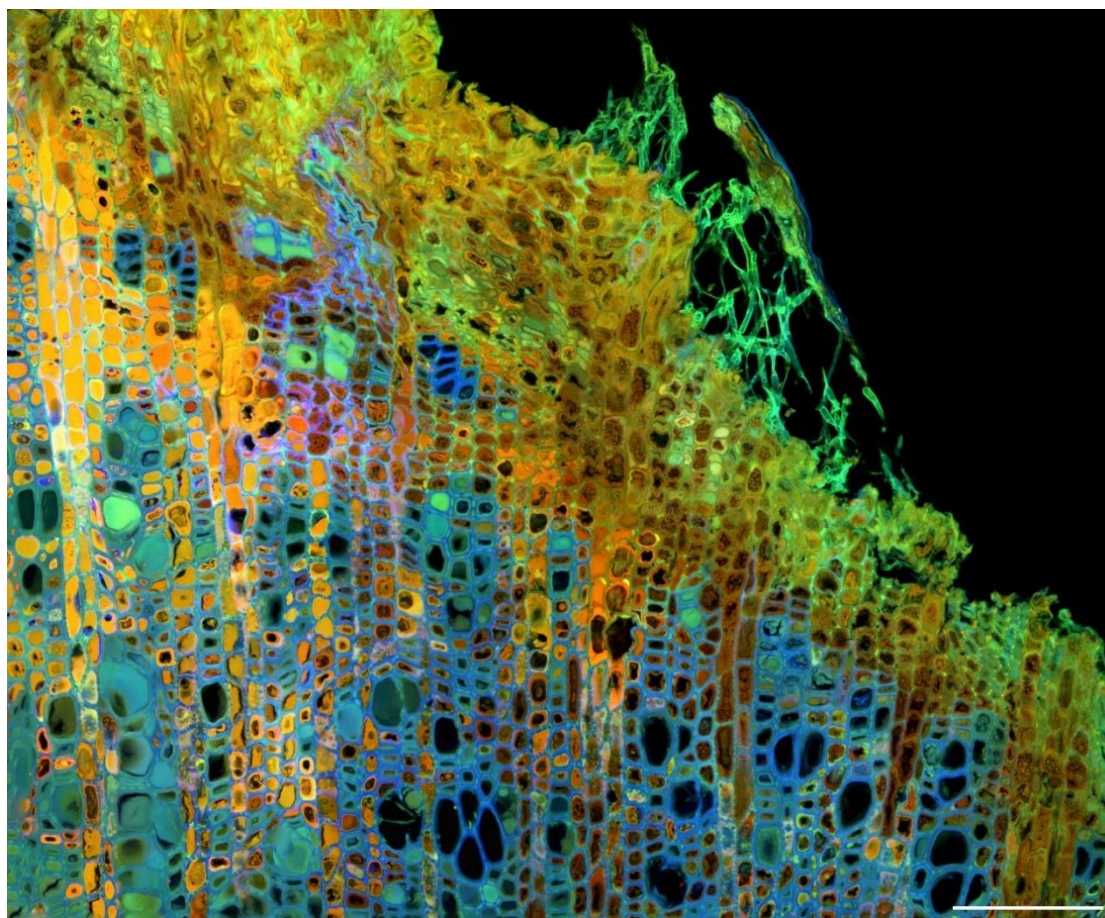
Figure 11. Spectral imaging of autofluorescence in a diseased apple stem (*Nectria* canker) using sequential excitation with emission ranges centered around the λ_{max} for each excitation wavelength. Excitation at 355 nm (UV), 488 nm (blue), and 561 nm (green). Many different unidentified fluorophores are present. However, blue cell walls represent lignin. Scale bar = 100 μm.

8.2. Unmixing

An alternative method to spatially localize multiple fluorophores in plant tissue is to perform spectral unmixing on a spectral sequence (a series of images acquired at small wavelength intervals using a single excitation wavelength) (Figure 12). This can be done either by using standard reference spectra or by using blind deconvolution algorithms [93], and in practice, these give essentially identical results. This usually works best with only a single excitation wavelength although sequential lambda sequences can be combined. This can potentially allow identification and localization of multiple fluorophores of the same color—two green fluorophores, for example, provided they have slightly different spectral characteristics. This technique has been used to localize different lignin types in poplar wood, where the fluorophores both have green emission with small differences in λ_{max} and relative intensity [32].
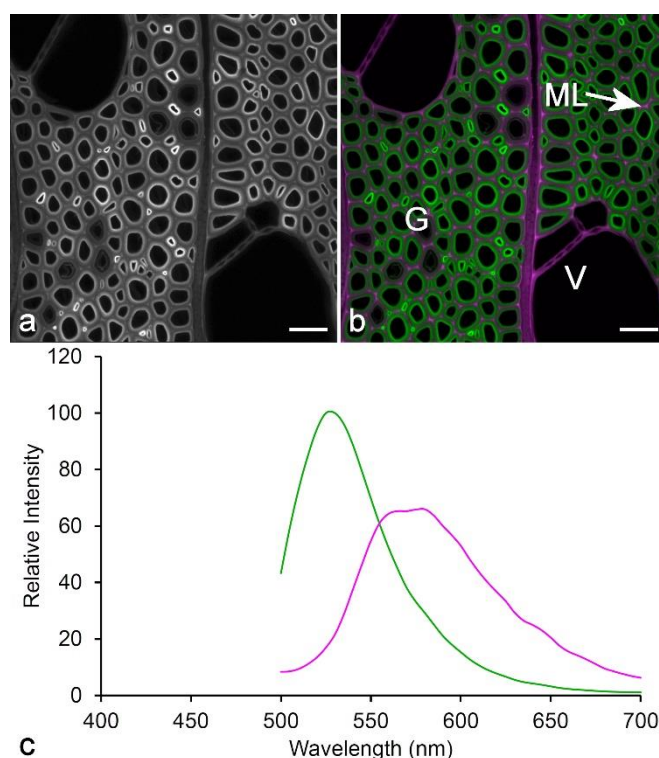
Figure 12. Spectral unmixing using Poisson NMF in ImageJ software [93]. (**a**) Poplar wood showing monochromatic lignin fluorescence (excitation at 488 nm, emission at 500–700 nm). Scale bar = 30 μm. (**b**) Poplar wood showing two-channel spectral unmixing calculated using Poisson NMF from a spectral image sequence (excitation at 488 nm, emission at 500–700 nm in 5 nm steps). The crimson regions correspond to areas rich in guaiacyl lignin (vessel cell walls [V] and middle lamella [ML]), while the green regions are rich in syringyl lignin (fiber secondary cell walls). The darker fibers (G) are gelatinous fibers (reaction wood) with weakly lignified cell walls. Scale bar = 30 μm. (**c**) Spectra calculated by blind unmixing using Poisson NMF [32,93]. The use of green and crimson for two-channel overlays is an alternative to green and red to accommodate color-blind readers.

Because chlorophyll fluorescence can interfere with imaging of expression tags such as fluorescent proteins, or other stains including immunolabeling, spectral unmixing can be used to isolate the chlorophyll fluorescence, allowing more precise localization of the tag or stain [94].

9. F-Techniques Using Autofluorescence

9.1. Fluorescence Lifetime Spectroscopy (FLIM)

FLIM offers an alternative to fluorescence intensity as a way of imaging the autofluorescence of plant tissues. Fluorescence lifetime (τ_m) is the time in picoseconds or nanoseconds between excitation of the fluorophore and its subsequent emission and is usually measured using time-correlated single-photon counting (TCSPC) [95].

Multiphoton FLIM has been used to study secondary metabolites in *Eucalyptus* secretory cavities [96]. Because sectioning results in damage to cells and subsequent loss of vacuolar contents, the use of multiphoton microscopy with its greater depth penetration allowed imaging of cellular contents up to 80 μm into the secretory structures. Secretory cavities contained autofluorescent oleuropeic acid glucose esters (τ_m = 1.4–1.5 ns) as well as non-fluorescent essential oils. Cell walls contained autofluorescent components with much shorter lifetimes—possibly ferulate or flavins.

Fluorescence lifetime imaging has also been used to detect anthocyanins in different cellular compartments using an anthocyanin-free mutant as a negative control [27]. Anthocyanins located

in vacuoles had shorter lifetimes compared to those in the cytoplasm and this was associated with a lower pH in the vacuole [27].

Fluorescence lifetime has been used in many studies on chlorophyll fluorescence and photosynthesis in algae and in higher plants [97,98]. In *Chlamydomonas*, changes in chlorophyll fluorescence lifetime were observed in zeaxanthin-accumulating mutants associated with the photoprotection function of these pigments. Zeaxanthin pigments quench chlorophyll fluorescence in a process that probably involves FRET [99,100]. Measurements of lifetime have been used to understand the various components of chlorophyll fluorescence in relation to photosystems I and II and to assign such components to fluorophore structures within the chlorophyll molecule [101]. Other applications include assessment of disease states [102], desiccation [103], and heavy metal toxicity [104].

Imaging and spectroscopy have been used to determine the fluorescence lifetime of wood lignin and to study its variation between cell wall layers and among wood types [105]. Lignin has a relatively short lifetime in the range of a few hundred picoseconds (Figure 13). There is a unimodal spectrum in normal wood and a bimodal spectrum in compression wood, which reflects the distribution of H-lignin in the middle lamella of normal wood and in the secondary wall of compression wood. The differentiation of G and H-lignins is somewhat greater by lifetime compared to intensity. Changes in lignin composition based on CAD mutants in *Arabidopsis*, where alcohol monomers are replaced with aldehydes have been shown to result in a change in fluorescence lifetime correlated to changes in composition determined by Raman spectroscopy [58]. Fluorescence lifetime has also been used in studies of pretreated woody biomass where changes in lifetime can be related to chemical pretreatments that influence amenability to enzymatic digestion for biofuel production [54,57]. FLIM has a lot of potential for plant autofluorescence applications, as it can potentially reveal differences that are much less obvious or not apparent in fluorescence intensity images. Lifetime is independent of intensity.
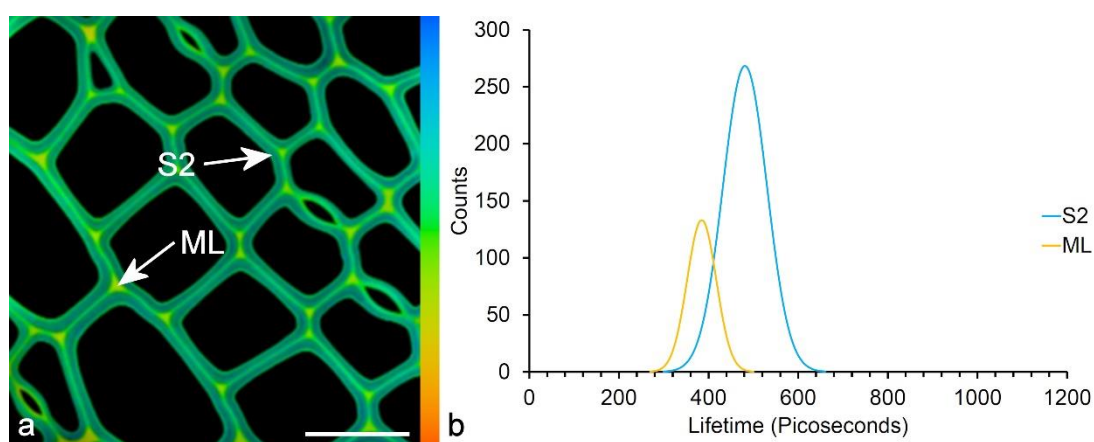
Figure 13. Fluorescence lifetime of pine lignin. (**a**) TS of pine wood showing a difference in fluorescence lifetime between the middle lamella (ML) and the secondary wall (S2). (Excitation at 405 nm.) Scale bar = 30 μm. Lifetime color scale from 0 to 1000 ps. (**b**) Fluorescence lifetime spectrum of the middle lamella (ML) compared to the secondary cell wall (S2) showing a shorter lifetime [105].

9.2. Förster Resonance Energy Transfer (FRET)

FRET is a method for measuring molecular interaction between two fluorophores with overlapping excitation and emission spectra. FRET occurs when a donor fluorophore and an acceptor fluorophore are in close proximity (<10 nm), making possible a non-radiative transfer of excitation energy from the donor to the acceptor. Typically, this technique is used to measure interaction between two labeled proteins where the labels form a FRET pair [106]. FRET is measured by determining the change in fluorescence intensity of the donor and/or acceptor, or the change in fluorescence lifetime of the donor in the presence or absence of the acceptor. Autofluorescence may be a hindrance to studies involving

FRET between dyes or endogenous expression tags such as GFP in plant cells [94,107]. Chlorophyll is especially problematic due to its bright fluorescence and wide range of excitation [94].

FRET between an autofluorescent donor and a dye-based acceptor has been described for wood and wood-based biomaterials [14,50,52,55]. Lignin and rhodamine form a FRET pair, with lignin as donor and rhodamine as acceptor, as determined by acceptor photobleaching [55] and FLIM [57]. Lignin autofluorescence with 458 nm excitation does not contribute any bleed through to emission from rhodamine excited at 561 nm and hence the two fluorophores can easily be distinguished, rhodamine fluorescence being very much brighter than lignin autofluorescence in the same emission range. FRET has been used to measure the accessibility of cell walls to rhodamine dye either when the cell wall is infiltrated with extractives as in heartwood [14], or when cell wall-based biomass has been pretreated to increase its porosity for enzymatic conversion of cellulose [52,55]. These studies have shown that lignin is less accessible to rhodamine in cell walls infiltrated with heartwood extractives [14]. More lignified regions of the cell wall (middle lamella) are less porous than those that are less lignified (secondary wall) [50,55]. There are some indications that lignin autofluorescence and extractive autofluorescence can also interact by FRET [14].

9.3. Colocalization

Colocalization can involve the use of various statistical measures to quantitatively assess the tendency for fluorophores to be at the same locations in tissues [108]. Lignin autofluorescence has been used to colocalize lignin with other cell wall components such as hemicelluloses detected by immunolocalization [34] or with fluorescently labeled enzymes for biotechnology applications [56].

10. Conclusions

Plants contain a wide array of autofluorescent molecules such as pigments, secretory compounds, or structural components of cell walls. Autofluorescence has applications in measuring the physiological status of crops or experimental plots based on measurements of chlorophyll fluorescence, and in imaging studies with applications in plant biochemistry, physiology, pathology, wood science, and plant biotechnology. Combining autofluorescence, including both intensity and lifetime imaging and spectroscopy, with other spectroscopic techniques such as Raman microspectroscopy and Fourier transform infra-red microspectroscopy (FTIR microscopy) may allow more accurate characterization of tissue fluorescence in plants at the cellular level in future studies [13,58]. Applications for using autofluorescence in techniques such as FRAP and FCS, which are used to track the diffusion of molecules in cells, may be forthcoming in the near future.

Conflicts of Interest: The author declares no conflict of interest.

References

1. García-Plazaola, J.I.; Fernández-Marína, B.; Duke, S.O.; Hernández, A.; López-Arbeloa, F.; Becerril, J.M. Autofluorescence: Biological functions and technical applications. *Plant Sci.* **2015**, *236*, 136–145. [CrossRef]
2. Dumur, T.; Duncan, S.; Graumann, K.; Desset, S.; Randall, R.S.; Scheid, O.M.; Bass, H.W.; Prodanov, D.; Tatout, C.; Baroux, C. Probing the 3D architecture of the plant nucleus with microscopy approaches: Challenges and solutions. *Nucleus* **2019**, *10*, 181–212. [CrossRef]
3. Kodama, Y. Time gating of chloroplast autofluorescence allows clearer fluorescence imaging in planta. *PLoS ONE* **2016**, *11*, e0152484. [CrossRef]

4.　Müller, S.M.; Galliardt, H.; Schneider, J.; Barisas, B.G.; Seidel, T. Quantification of Förster resonance energy transfer by monitoring sensitized emission in living plant cells. *Front. Plant Sci.* **2013**, *4*, 413. [CrossRef]

5.　Buschmann, C.; Langsdorf, G.; Lichtenthaler, H.K. Imaging of the blue, green, and red fluorescence emission of plants: An overview. *Photosynthetica* **2000**, *38*, 483–491. [CrossRef]

6.　Cerovic, Z.G.; Samson, G.; Morales, F.; Tremblay, N.; Moya, I. Ultraviolet-induced fluorescence for plant monitoring: Present state and prospects. *Agronomie* **1999**, *19*, 543–578. [CrossRef]

7.　Roshchina, V.V. Vital autofluorescence: Application to the study of plant living cells. *Int. J. Spectrosc.* **2012**, 1–14. [CrossRef]

8.　Roshchina, V.V. Autofluorescence of plant secreting cells as a biosensor and bioindicator reaction. *J. Fluoresc.* **2003**, *13*, 403–426. [CrossRef]

9.　Roshchina, V.V.; Yashin, V.A.; Kononov, A.V. Autofluorescence of developing plant vegetative microspores studied by confocal microscopy and microspectrofluorimetry. *J. Fluoresc.* **2004**, *14*, 745–750. [CrossRef]

10.　Roshchina, V.V.; Kuchin, A.V.; Yashin, V.A. Application of autofluorescence for analysis of medicinal plants. *Int. J. Spectrosc.* **2017**, 1–8. [CrossRef]

11.　Rost, F.W.D. Autofluorescence in plants, fungi, and bacteria. In *Fluorescence Microscopy*; Rost, F.W.D., Ed.; Cambridge University Press: Cambridge, UK, 1995; Volume 2, pp. 16–36.

12.　Talamond, P.; Verdeil, J.-L.; Conéjéro, G. Secondary metabolite localization by autofluorescence in living plant cells. *Molecules* **2015**, *20*, 5024–5037. [CrossRef]

13.　Mottiar, Y.; Gierlinger, N.; Jeremic, D.; Master, E.R.; Mansfield, S.D. Atypical lignification in eastern leatherwood (*Dirca palustris*). *New Phytol.* **2020**. [CrossRef]

14.　Donaldson, L.A.; Singh, A.; Raymond, L.; Hill, S.; Schmitt, U. Extractive distribution in *Pseudotsuga menziesii*: Effects on cell wall porosity in sapwood and heartwood. *IAWA J.* **2019**, *40*, 721–740. [CrossRef]

15.　Donaldson, L.; Williams, N. Imaging and spectroscopy of natural fluorophores in pine needles. *Plants* **2018**, *7*, 10. [CrossRef]

16.　Lamb, J.J.; Røkke, G.; Hohmann-Marriott, M.F. Chlorophyll fluorescence emission spectroscopy of oxygenic organisms at 77 K. *Photosynthetica* **2018**, *56*, 105–124. [CrossRef]

17.　Mohammed, G.H.; Colombo, R.; Middleton, E.M.; Rascher, U.; Van der Tol, C.; Nedbal, L.; Goulas, Y.; Pérez-Priego, O.; Damm, A.; Meroni, M.; et al. Remote sensing of solar-induced chlorophyll fluorescence (SIF) in vegetation: 50 years of progress. *Remote Sens. Environ.* **2019**, *231*, 111177. [CrossRef]

18.　Forster, L.S.; Livingston, R. The absolute quantum yields of the fluorescence of chlorophyll solutions. *J. Chem. Phys.* **1952**, *20*, 1315–1320. [CrossRef]

19.　Vácha, F.; Sarafis, V.; Benediktyová, Z.; Bumba, L.; Valenta, J.; Vácha, M.; Sheue, C.-R.; Nedbal, L. Identification of photosystem I and photosystem II enriched regions of thylakoid membrane by optical microimaging of cryo-fluorescence emission spectra and of variable fluorescence. *Micron* **2007**, *38*, 170–175. [CrossRef]

20.　Yamamoto, Y.; Hori, H.; Kai, S.; Ishikawa, T.; Ohnishi, A.; Tsumura, N.; Morita, N. Quality control of photosystem II: Reversible and irreversible protein aggregation decides the fate of photosystem II under excessive illumination. *Front. Plant Sci.* **2013**, *4*, 433. [CrossRef]

21.　Baker, N.R. Chlorophyll fluorescence: A probe of photosynthesis in vivo. *Annu. Rev. Plant Biol.* **2008**, *59*, 89–113. [CrossRef]

22.　Galbraith, D.W.; Harkins, K.R.; Jefferson, R.A. Flow cytometric characterization of the chlorophyll contents and size distributions of plant protoplasts. *Cytometry* **1988**, *9*, 75–83. [CrossRef]

23.　Guanter, L.; Zhang, Y.; Jung, M.; Joiner, J.; Voigt, M.; Berry, J.A.; Frankenberg, C.; Huete, A.R.; Zarco-Tejada, P.; Lee, J.-E.; et al. Global and time-resolved monitoring of crop photosynthesis with chlorophyll fluorescence. *Proc. Natl. Acad. Sci. USA* **2014**, E1327–E1333. [CrossRef]

24.　Maxwell, K.; Johnson, G.N. Chlorophyll fluorescence—A practical guide. *J. Exp. Bot.* **2000**, *51*, 659–668. [CrossRef]

25.　Murchie, E.H.; Lawson, T. Chlorophyll fluorescence analysis: A guide to good practice and understanding some new applications. *J. Exp. Bot.* **2013**, *64*, 3983–3998. [CrossRef]

26.　Drabent, R.; Pliszka, B.; Olzewska, T. Fluorescence properties of plant anthocyanin pigments. I Fluorescence of anthocyanins in *Brassica oleracea* L. extracts. *J. Photochem. Photobiol.* **1999**, *50*, 53–58. [CrossRef]

27.　Chanoca, A.; Burkel, B.; Kovinich, N.; Grotewold, E.; Eliceiri, K.W.; Otegui, M.S. Using fluorescence lifetime microscopy to study the subcellular localization of anthocyanins. *Plant J.* **2016**, *88*, 895–903. [CrossRef]

28. Zaghdoudi, K.; Ngomo, O.; Vanderesse, R.; Arnoux, P.; Myrzakhmetov, B.; Frochot, C.; Guiavarc'h, Y. Extraction, identification and photo-physical characterization of persimmon (*Diospyros kaki* L.) carotenoids. *Foods* **2017**, *6*, 4. [CrossRef]

29. Merzlyak, M.N.; Melø, T.B.; Naqvi, K.R. Effect of anthocyanins, carotenoids, and flavonols on chlorophyll fluorescence excitation spectra in apple fruit: Signature analysis, assessment, modeling, and relevance to photoprotection. *J. Exp. Bot.* **2008**, *59*, 349–359. [CrossRef]

30. Kleinegris, D.M.M.; Van Es, M.A.; Janssen, M.; Brandenburg, W.A.; Wijffels, R.H. Carotenoid fluorescence in *Dunaliella salina*. *J. Appl. Phycol.* **2010**, *22*, 645–649. [CrossRef]

31. Castellan, A.; Ruggiero, R.; Frollini, E.; Ramos, L.A.; Chirat, C. Studies on fluorescence of cellulosics. *Holzforschung* **2007**, *61*, 504–508. [CrossRef]

32. Donaldson, L.A. Softwood and hardwood lignin fluorescence spectra of wood cell walls in different mounting media. *IAWA J.* **2013**, *34*, 3–19. [CrossRef]

33. Hafren, J. Excitation wavelength-specific changes in lignocellulosic autofluorescence. *J. Wood Sci.* **2007**, *53*, 358–360. [CrossRef]

34. Donaldson, L.A.; Knox, J.P. Localisation of cell wall polysaccharides in normal and compression wood of radiata pine—Relationships with lignification and microfibril orientation. *Plant Physiol.* **2012**, *158*, 642–653. [CrossRef]

35. Donaldson, L.A.; Radotić, K.; Kalauzi, A.; Djikanović, D.; Jeremić, M. Quantification of compression wood severity in tracheids of *Pinus radiata* D. Don using confocal fluorescence imaging and spectral deconvolution. *J. Struct. Biol.* **2010**, *169*, 106–115. [CrossRef]

36. Radotić, K.; Kalauzi, A.; Djikanović, D.; Jeremić, M.; Leblanc, R.M.; Cerović, Z.G. Component analysis of the fluorescence spectra of a lignin model compound. *J. Photochem. Photobiol. B Biol.* **2006**, *83*, 1–10. [CrossRef]

37. Albinsson, B.; Li, S.; Lundquist, K.; Stomberg, R. The origin of lignin fluorescence. *J. Mol. Struct.* **1999**, *508*, 19–27. [CrossRef]

38. Castellan, A.; Davidson, R.S. Steady-state and dynamic fluorescence emission from *Abies* wood. *J. Photochem. Photobiol. A Chem.* **1994**, *78*, 275–279. [CrossRef]

39. Lundquist, K.; Josefsson, B.; Nyquist, G. Analysis of lignin products by fluorescence spectroscopy. *Holzforshung* **1978**, *32*, 27–32. [CrossRef]

40. Xue, Y.; Qiu, X.; Wu, Y.; Qian, Y.; Zhou, M.; Deng, Y.; Li, Y. Aggregation-induced emission: The origin of lignin fluorescence. *Polym. Chem.* **2016**, *7*, 3502–3508. [CrossRef]

41. Donaldson, L.A.; Kroese, H.W.; Hill, S.J.; Franich, R.A. Detection of wood cell wall porosity using small carbohydrate molecules and confocal fluorescence microscopy. *J. Microsc.* **2015**, *259*, 228–236. [CrossRef]

42. Kim, J.S.; Gao, J.; Terziev, N.; Cuccui, I.; Daniel, G. Chemical and ultrastructural changes of ash wood thermally modified using the thermo-vacuum process: I. Histo/cytochemical studies on changes in the structure and lignin chemistry. *Holzforschung* **2015**, *69*, 603–613. [CrossRef]

43. Thygesen, L.G.; Barsberg, S.; Venås, T.M. The fluorescence characteristics of furfurylated wood studied by fluorescence spectroscopy and confocal laser scanning microscopy. *Wood Sci. Technol.* **2010**, *44*, 51–65. [CrossRef]

44. Irbe, I.; Noldt, G.; Koch, G.; Andersone, I.; Andersons, B. Application of scanning UV microspectrophotometry for the topochemical detection of lignin within individual cell walls of brown-rotted Scots pine (*Pinus sylvestris* L.) sapwood. *Holzforschung* **2006**, *60*, 601–607. [CrossRef]

45. Cox, G.; Moreno, N. Second-harmonic imaging of plant polysaccharides. *J. Biomed. Opt.* **2005**, *10*, 024013. [CrossRef]

46. Kushida, S.; Braam, D.; Pan, C.; Dao, T.D.; Tabata, K.; Sugiyasu, K.; Takeuchi, M.; Ishii, S.; Nagao, T.; Lorke, A.; et al. Whispering gallery resonance from self-assembled microspheres of highly fluorescent isolated conjugated polymers. *Macromolecules* **2015**, *48*, 3928–3933. [CrossRef]

47. Wagner, A.; Donaldson, L.A.; Kim, H.; Phillips, L.; Flint, H.; Steward, D.; Torr, K.; Koch, G.; Schmitt, U.; Ralph, J. Silencing of 4-coumarate-CoA ligase in the coniferous gymnosperm *Pinus radiata*. *Plant Physiol.* **2008**, *149*, 370–383. [CrossRef]

48. Donaldson, L.A.; Grace, J.C.; Downes, G. Within tree variation in anatomical properties of compression wood in radiata pine. *IAWA J.* **2004**, *25*, 253–271. [CrossRef]

49.　Donaldson, L.A.; Nanayakkara, B.; Radotić, K.; Djikanovic-Golubovic, D.; Mitrovic, A.; Bogdanovic, J.; Simonovic, J.; Kalauzi, A. Xylem parenchyma cell walls lack a gravitropic response in conifer compression wood. *Planta* **2015**, *242*, 1413–1424. [CrossRef]

50.　Donaldson, L.A.; Cairns, M.; Hill, S.J. Comparison of micropore distribution in cell walls of softwood and hardwood xylem. *Plant Physiol.* **2018**, *178*, 1142–1153. [CrossRef]

51.　Auxenfans, T.; Terryn, C.; Paës, G. Seeing biomass recalcitrance through fluorescence. *Sci. Rep.* **2017**, *7*, 8838. [CrossRef]

52.　Chabbert, B.; Terryn, C.; Herbaut, M.; Vaidya, A.; Habrant, A.; Paës, G.; Donaldson, L. Fluorescence techniques can reveal cell wall organization and predict saccharification in pretreated wood biomass. *Ind. Crops. Prod.* **2018**, *123*, 84–92. [CrossRef]

53.　Chimenez, T.A.; Gehlen, M.H.; Marabezi, K.; Curvelo, A.A.S. Characterization of sugarcane bagasse by autofluorescence microscopy. *Cellulose* **2014**, *21*, 653–664. [CrossRef]

54.　Coletta, V.C.; Rezende, C.A.; Da Conceição, F.A.; Polikarpov, I.; Guimarães, F.E.G. Mapping the lignin distribution in pretreated sugarcane bagasse by confocal and fluorescence lifetime imaging microscopy. *Biotechnol. Biofuels* **2013**, *6*, 43. [CrossRef] [PubMed]

55.　Donaldson, L.A.; Newman, R.H.; Vaidya, A. Nanoscale interactions of polyethylene glycol with thermo-mechanically pre-treated *Pinus radiata* biofuel substrate. *Biotechnol. Bioeng.* **2014**, *111*, 719–725. [CrossRef]

56.　Donaldson, L.A.; Vaidya, A. Visualising recalcitrance by colocalization of cellulase, lignin and cellulose in pretreated pine biomass using fluorescence microscopy. *Sci. Rep.* **2017**, *7*, 44386. [CrossRef]

57.　Terryn, C.; Paës, G.; Spriet, C. FRET-SLiM on native autofluorescence: A fast and reliable method to study interactions between fluorescent probes and lignin in plant cell wall. *Plant Methods* **2018**, *14*, 74. [CrossRef]

58.　Wightman, R.; Busse-Wicher, M.; Dupree, P. Correlative FLIM-confocal-Raman mapping applied to plant lignin composition and autofluorescence. *Micron* **2019**, *126*, 102733. [CrossRef]

59.　Zeng, Y.; Zhao, S.; Wei, H.; Tucker, M.P.; Himmel, M.E.; Mosier, N.S.; Meilan, R.; Ding, S.-Y. In situ micro-spectroscopic investigation of lignin in poplar cell walls pretreated by maleic acid. *Biotechnol. Biofuels* **2015**, *8*, 126. [CrossRef]

60.　Harris, P.J.; Hartley, R.D. Detection of bound ferulic acid in cell walls of the Gramineae by ultraviolet fluorescence microscopy. *Nature* **1976**, *259*, 508–510. [CrossRef]

61.　Cappelli, A.; Paolino, M.; Reale, A.; Razzano, V.; Grisci, G.; Giuliani, G.; Donati, A.; Bonechi, C.; Lamponi, S.; Mendichi, R.; et al. Hyaluronan-based graft copolymers bearing aggregation-induced emission fluorogens. *RSC Adv.* **2018**, *8*, 5864–5881. [CrossRef]

62.　Carnachan, S.M.; Harris, P.J. Ferulic acid is bound to the primary cell walls of all gymnosperm families. *Biochem. Syst. Ecol.* **2000**, *28*, 865–879. [CrossRef]

63.　Berg, R.H. Evaluation of spectral imaging for plant cell analysis. *J. Microsc.* **2004**, *214*, 174–181. [CrossRef]

64.　Buda, G.J.; Isaacson, T.; Matas, A.J.; Paolillo, D.J.; Rose, J.K.C. Three-dimensional imaging of plant cuticle architecture using confocal scanning laser microscopy. *Plant J.* **2009**, *60*, 378–385. [CrossRef]

65.　Fernández, S.; Osorio, S.; Heredia, A. Monitoring and visualising plant cuticles by confocal laser scanning microscopy. *Plant Physiol. Biochem.* **1999**, *37*, 789–794. [CrossRef]

66.　Philippe, G.; Sørensen, I.; Jiao, C.; Sun, X.; Fei, Z.; Domozych, D.S.; Rose, J.K.C. Cutin and suberin: Assembly and origins of specialized lipidic cell wall scaffolds. *Curr. Opin. Plant Biol.* **2020**, *55*, 11–20. [CrossRef] [PubMed]

67.　Correia, V.G.; Bento, A.; Pais, J.; Rodrigues, R.; Haliński, Ł.P.; Frydrych, M.; Greenhalgh, A.; Stepnowski, P.; Vollrath, F.; King, A.W.T.; et al. The molecular structure and multifunctionality of the cryptic plant polymer suberin. *Mater. Today Bio* **2020**, *5*, 100039. [CrossRef] [PubMed]

68.　Li, F.-S.; Phyo, P.; Jacobowitz, J.; Hong, M.; Weng, J.-K. The molecular structure of plant sporopollenin. *Nat. Plants* **2019**, *5*, 41–46. [CrossRef] [PubMed]

69.　Willemse, M.T.M. Changes in the autofluorescence of the pollen wall during microsporogenesis and chemical treatments. *Acta Bot. Neerl.* **1972**, *21*, 1–16. [CrossRef]

70.　Roshchina, V.V.; Melnikova, E.V.; Iashin, V.A.; Kamaukhov, V.N. Autofluorescence of intact *Equisetum arvense* L. spores during their development. *Biofizika* **2002**, *47*, 318–324. (In Russian)

71. Castro, A.J.; Rejón, J.D.; Fendri, M.; Jiménez-Quesada, M.J.; Zafra, A.; Jiménez-López, J.C.; Rodríguez-García, M.I.; Alché, J.D. Taxonomical discrimination of pollen grains by using confocal laser scanning microscopy (CLSM) imaging of autofluorescence. In *Microscopy: Science, Technology, Applications and Education*; Méndez-Vilas, A., Díaz, J., Eds.; Formatex: Badajoz, Spain, 2010; pp. 607–613.

72. Urbanczyk, J.; Casado, M.A.F.; Díaz, T.E.; Heras, P.; Infante, M.; Borrego, A.G. Reprint of "Spectral fluorescence variation of pollen and spores from recent peat-forming plants". *Int. J. Coal Geol.* **2015**, *139*, 206–216. [CrossRef]

73. Acuña, A.U.; Amat-Guerri, F.; Morcillo, P.; Liras, M.; Rodriguez, B. Structure and formation of the fluorescent compound of *Lignum nephriticum*. *Org. Lett.* **2009**, *11*, 3020–3023. [CrossRef]

74. Schnitzler, J.-P.; Jungblut, T.P.; Heller, W.; Köfferlein, M.; Hutzler, P.; Heinzmann, U.; Schmelzer, E.; Ernst, D.; Langebartels, C.; Sandermann, H. Tissue localization of UV-B screening pigments and of chalcone synthase mRNA in needles of Scots pine seedlings. *New Phytol.* **1996**, *132*, 247–258. [CrossRef]

75. Weston, L.A.; Mathesius, U. Flavonoids: Their structure, biosynthesis and role in the rhizosphere, including allelopathy. *J. Chem. Ecol.* **2013**, *39*, 283–297. [CrossRef]

76. Hutzler, P.; Fischbach, R.; Heller, W.; Jungblut, T.P.; Reuber, S.; Schmitz, R.; Veit, M.; Weissenböck, G.; Schnitzler, J.-P. Tissue localization of phenolic compounds in plants by confocal laser scanning microscopy. *J. Exp. Bot.* **1998**, *49*, 953–965. [CrossRef]

77. Sudo, E.; Teranishi, M.; Hidema, J.; Taniuchi, T. Visualization of flavonol distribution in the abaxial epidermis of onion scales via detection of its autofluorescence in the absence of chemical processes. *Biosci. Biotechnol. Biochem.* **2009**, *73*, 2107–2109. [CrossRef]

78. Monago-Maraña, O.; Durán-Merás, I.; Galeano-Díaz, T.; De la Peña, A.M. Fluorescence properties of flavonoid compounds. Quantification in paprika samples using spectrofluorimetry coupled to second-order chemometric tools. *Food Chem.* **2016**, *196*, 1058–1065. [CrossRef]

79. Buer, C.S.; Muday, G.K. The *transparent testa4* mutation prevents flavonoid synthesis and alters auxin transport and the response of *Arabidopsis* roots to gravity and light. *Plant Cell* **2004**, *16*, 1191–1205. [CrossRef]

80. Peer, W.A.; Brown, D.E.; Tague, B.W.; Muday, G.K.; Taiz, L.; Murphy, A.S. Flavonoid accumulation patterns of *transparent testa* mutants of *Arabidopsis*. *Plant Physiol.* **2001**, *126*, 536–548. [CrossRef]

81. Bellow, S.; Latouche, G.; Brown, S.C.; Poutaraud, A.; Cerovic, Z.G. In vivo localization at the cellular level of stilbene fluorescence induced by *Plasmopara viticola* in grapevine leaves. *J. Exp. Bot.* **2012**, *63*, 3697–3708. [CrossRef]

82. Dubouzet, J.G.; Donaldson, L.; Black, M.A.; McNoe, L.; Liu, V.; Lloyd-Jones, G. Heterologous hybridization to a *Pinus* microarray: Profiling of gene expression in *Pinus radiata* saplings exposed to ethephon. *NZ J. For. Sci.* **2014**, *44*, 21–34. [CrossRef]

83. Mishra, G.; Collings, D.A.; Altaner, C.M. Cell organelles and fluorescence of parenchyma cells in *Eucalyptus bosistoana* sapwood and heartwood investigated by microscopy. *NZ J. For. Sci.* **2018**, *48*, 13. [CrossRef]

84. Brillouet, J.M.; Romieu, C.; Schoefs, B.; Solymosi, K.; Cheynier, V.; Fulcrand, H.; Verdeil, J.-L.; Conéjéro, G. The tannosome is an organelle forming condensed tannins in the chlorophyllous organs of tracheophyta. *Ann. Bot.* **2013**, *112*, 1003–1014. [CrossRef]

85. Engelbrecht, L.; Frazenburg, M.; Laurie, A. The South African persimmon under the microscope. *S. Afr. Fruit J.* **2019**, *18*, 53–55.

86. Binsch, G.; Heilbronner, E.; Jankow, R.; Schmidt, D. On the fluorescence anomaly of azulene. *Chem. Phys. Lett.* **1967**, *1*, 135–138. [CrossRef]

87. Collins, J.S.; Goldsmith, T.H. Spectral properties of fluorescence induced by glutaraldehyde fixation. *J. Histochem. Cytochem.* **1981**, *29*, 411–414. [CrossRef]

88. Prior, D.A.M.; Oparka, K.J.; Roberts, I.M. En-bloc optical sectioning of resin-embedded specimens using a confocal laser scanning microscope. *J. Microsc.* **1999**, *193*, 20–27. [CrossRef]

89. Wu, C.H.; Warren, H.L. Natural autofluorescence in fungi and its correlation with viability. *Mycologia* **1984**, *76*, 1049–1058. [CrossRef]

90. Culley, S.; Kalina, L.; Tosheva, K.L.; Pereira, P.M.; Henriques, R. SRRF: Universal live-cell super-resolution microscopy. *Int. J. Biochem. Cell Biol.* **2018**, *101*, 74–79. [CrossRef]

91. Jamme, F.; Kascakova, S.; Villette, S.; Allouche, F.; Pallu, S.; Rouam, V.; Réfrégiers, M. DUV Autofluorescence microscopy for cell biology and tissue histology. *Biol. Cell.* **2013**, *105*, 277–288. [CrossRef]

92. Devaux, M.-F.; Jamme, F.; André, W.; Bouchet, B.; Alvarado, C.; Durand, S.; Robert, P.; Saulnier, L.; Bonnin, E.; Guillon, F. Synchrotron time-lapse imaging of lignocellulosic biomass hydrolysis: Tracking enzyme localization by protein autofluorescence and biochemical modification of cell walls by microfluidic infrared microspectroscopy. *Front. Plant Sci.* **2018**, *9*, 200. [CrossRef]

93. Neher, R.A.; Mitkovski, M.; Kirchhoff, F.; Neher, E.; Theis, F.J.; Zeug, A. Blind source separation techniques for the decomposition of multiply labeled fluorescence images. *Biophys. J.* **2009**, *96*, 3791–3800. [CrossRef] [PubMed]

94. Berg, R.H.; Beachy, R.N. Fluorescent protein applications in plants. *Method. Cell Biol.* **2008**, *85*, 153–177. [CrossRef]

95. Wahl, M. *Time-Correlated Single-Photon Counting*; Picoquant Technical Note: Berlin, Germany, 2014; pp. 1–14.

96. Heskes, A.M.; Lincoln, C.N.; Goodger, J.Q.D.; Woodrow, I.E.; Smith, T.A. Multiphoton fluorescence lifetime imaging shows spatial segregation of secondary metabolites in *Eucalyptus* secretory cavities. *J. Microsc.* **2012**, *247*, 33–42. [CrossRef]

97. Brody, S.S. Fluorescence lifetime, yield, energy transfer and spectrum in photosynthesis, 1950-1960. In *Discoveries in Photosynthesis*; Govindjee, Beatty, J.T., Gest, H., Allen, J.F., Eds.; Advances in Photosynthesis and Respiration; Springer: Dordrecht, The Netherlands, 2005; Volume 20, pp. 165–170. [CrossRef]

98. Holub, O.; Seufferheld, M.J.; Gohlke, C.; Govindjee; Clegg, R.M. Fluorescence lifetime imaging (FLI) in real-time—A new technique in photosynthesis research. *Photosynthetica* **2000**, *38*, 581–599. [CrossRef]

99. Amarnath, K.; Zaks, J.; Park, S.D.; Niyogi, K.K.; Fleming, G.R. Fluorescence lifetime snapshots reveal two rapidly reversible mechanisms of photoprotection in live cells of *Chlamydomonas reinhardtii*. *Proc. Natl. Acad. Sci. USA* **2012**, *109*, 8405–8410. [CrossRef]

100. Holub, O.; Seufferheld, M.J.; Gohlke, C.; Govindjee; Heiss, G.J.; Clegg, R.M. Fluorescence lifetime imaging microscopy of *Chlamydomonas reinhardtii*: Non-photochemical quenching mutants and the effect of photosynthetic inhibitors on the slow chlorophyll fluorescence transient. *J. Microsc.* **2007**, *226*, 90–120. [CrossRef]

101. Moise, N.; Moya, I. Correlation between lifetime heterogeneity and kinetics heterogeneity during chlorophyll fluorescence induction in leaves: 2. Multi-frequency phase and modulation analysis evidences a loosely connected PSII pigment-protein complex. *Biochim. Biophys. Acta* **2004**, *1657*, 47–60. [CrossRef]

102. Lei, R.; Jiang, H.; Hu, F.; Yan, J.; Zhu, S. Chlorophyll fluorescence lifetime imaging provides new insight into the chlorosis induced by plant virus infection. *Plant Cell Rep.* **2017**, *36*, 327–341. [CrossRef]

103. Bilger, W. Desiccation-induced quenching of chlorophyll fluorescence in cryptogams. In *Non-Photochemical Quenching and Energy Dissipation in Plants, Algae and Cyanobacteria*; Demmig-Adams, B., Garab, G., Adams, W., III, Govindjee, Eds.; Advances in Photosynthesis and Respiration (Including Bioenergy and Related Processes); Springer: Dordrecht, The Netherlands, 2014; Volume 40, pp. 409–420. [CrossRef]

104. Zeng, Y.; Wu, Y.; Li, D.; Zheng, W.; Wang, W.-X.; Qu, J.Y. Two-photon excitation chlorophyll fluorescence lifetime imaging: A rapid and non-invasive method for in vivo assessment of cadmium toxicity in a marine diatom *Thalassiosira weissflogii*. *Planta* **2012**, *236*, 1653–1663. [CrossRef]

105. Donaldson, L.A.; Radotic, K. Fluorescence lifetime imaging of lignin autofluorescence in normal and compression wood. *J. Microsc.* **2013**, *251*, 178–187. [CrossRef]

106. Periasamy, A.; Day, R.N. *Molecular Imaging, FRET Microscopy and Spectroscopy*; Oxford University Press: New York, NY, USA, 2005; p. 312. [CrossRef]

107. Weidtkamp-Peters, S.; Stahl, Y. The use of FRET/FLIM to study proteins interacting with plant receptor kinases. In *Plant Receptor Kinases*; Aalen, R., Ed.; Methods in Molecular Biology; Humana Press: New York, NY, USA, 2017; Volume 1621, pp. 163–175. [CrossRef]

108. Bolte, S.; Cordelières, F.P. A guided tour into subcellular colocalization analysis in light microscopy. *J. Microsc.* **2006**, *224*, 213–232. [CrossRef]